ORNL/TM-2022/2548

Experimental Determination of Constitutive Response of Alloy 800H in Support of Viscoplastic Constitutive Model Development for ASME Section III, Division 5, Class A Applications

Yanli Wang
Peijun Hou

August 2022

OAK RIDGE National Laboratory

ORNL IS MANAGED BY UT-BATTELLE LLC FOR THE US DEPARTMENT OF ENERGY

ORNL/TM-2022/2548

Materials Science and Technology Division

EXPERIMENTAL DETERMINATION OF CONSTITUTIVE RESPONSE OF ALLOY 800H IN SUPPORT OF VISCOPLASTIC CONSTITUTIVE MODEL DEVELOPMENT FOR ASME SECTION III, DIVISION 5, CLASS A APPLICATIONS

Yanli Wang
Peijun Hou[1]

[1] Imtech Corporation, Knoxville

Date Published: August 2022

Prepared by
OAK RIDGE NATIONAL LABORATORY
Oak Ridge, TN 37831
managed by
UT-BATTELLE LLC
for the
US DEPARTMENT OF ENERGY
under contract DE-AC05-00OR22725

CONTENTS

LIST OF FIGURES

LIST OF TABLES

ABBREVIATIONS

Argonne	Argonne National Laboratory
ART	Advanced Reactor Technologies
ASME	American Society of Mechanical Engineers
CF	creep-fatigue
DOE	US Department of Energy
DSA	dynamic strain aging
GCR	gas-cooled reactors
HTGR	high-temperature gas-cooled reactor
ORNL	Oak Ridge National Laboratory
RT	room temperature

ACKNOWLEDGMENTS

This research was sponsored by the US Department of Energy (DOE) under contract no. DE-AC05-00OR22725 with Oak Ridge National Laboratory (ORNL), managed and operated by UT-Battelle LLC. Programmatic direction was provided by the Office of Nuclear Reactor Deployment of the DOE Office of Nuclear Energy.

The authors gratefully acknowledge the support provided by Ting-Leung (Sam) Sham, Advanced Materials Technology Area Lead for the Advanced Reactor Technologies (ART) Program; Sue Lesica, Federal Materials Lead for the ART Program; Matthew Hahn, Federal Program Manager of the ART Gas-Cooled Reactors (GCR) Campaign; and Gerhard Strydom of Idaho National Laboratory, National Technical Director of the ART GCR Campaign.

The authors also wish to thank ORNL staff members C. Shane Hawkins for technical support and Lianshan Lin and Jian Chen for reviewing this report.

ABSTRACT

In FY 2022, a development effort was initiated at the US Department of Energy's Argonne National Laboratory (Argonne) and Oak Ridge National Laboratory (ORNL) to develop the Alloy 800H viscoplastic constitutive model so that inelastic analysis methods can support high-temperature gas-cooled reactor (HTGR) designs. The viscoplastic constitutive equations will be developed at Argonne. The ORNL effort focuses on generating test data from various high-temperature experiments with specially designed loading histories to probe Alloy 800H's constitutive response.

This report documents ORNL's experimental results on Alloy 800H in support of the development of the viscoplastic constitutive model. Specifically, the strain rate sensitivity, pure fatigue test to failure at various temperatures, cyclic stress–strain curves and creep-fatigue responses at 650°C and 750°C on Alloy 800H were investigated and are summarized in this report.

1. BACKGROUND

The use of inelastic analysis methods is the most accurate and least overconservative of the American Society of Mechanical Engineers (ASME) nuclear high-temperature design options. The Advanced Reactor Technologies (ART) Program has developed the viscoplastic constitutive models for Grade 91 steel, Type 316 stainless steel, and Alloy 617 to facilitate of the use of the inelastic analysis methods. In FY 2022, an effort was initiated at the US Department of Energy's Argonne National Laboratory (Argonne) and Oak Ridge National Laboratory (ORNL) to develop the Alloy 800H viscoplastic constitutive model. Alloy 800H is the reference construction material for high-temperature gas-cooled reactor (HTGR) designs. Development of a suitable viscoplastic constitutive model for Alloy 800H for use in Section III, Division 5 of the ASME Boiler and Pressure Vessel Code will lead to flexibility in using the design by inelastic analysis methods and will offer more efficient structural designs for advanced reactor developers.

Reviewing the available experimental data on Alloy 800H in literature for use in developing the viscoplastic constitutive model revealed a data gap, especially its mechanical responses to cyclic loading at various temperatures and to strain rate changes. ORNL is tasked with designing and performing experiments on Alloy 800H to probe the constitutive responses and fill the data gap. The following experiments were conducted: (1) strain-controlled strain rate jump tests at high temperatures of 600°C, 700°C and 800°C; (2) fatigue testing to failure at a temperature range from room temperature (RT) to 800°C; and (3) specifically designed fatigue and creep-fatigue (CF) tests at high temperatures of 650°C and 750°C. The results from these experiments are summarized in this report.

2. MATERIAL

Alloy 800H is an approved Class A material in the ASME code for nuclear applications up to 760°C and has a maximum design life of 300,000 h. The Alloy 800H material used in this study had a heat number of 37458 and was a historical reference plate material stored at ORNL. The plate was manufactured by Jessop Steel Company in 1989 and has a factory marking of UNS 08811, which indicates that it meets the ASTM B409-87 specification, an earlier version of ASTM B409-06 specification.

The chemical composition of the Alloy 800H and the ASTM B409-06 specifications are listed in Table 1. The combined content of Al and Ti is 0.88 wt %, which meets the minimum requirements of 0.50 wt % stipulated by ASME Section III, Division 5 Table HBB-I-14.1(a). Additionally, Wright et al. (2010) performed detailed characterization of this heat of Alloy 800H and reported that it meets the Alloy 800H specifications, including grain size and tensile properties.

Table 1. Chemical compositions of Alloy 800H (heat number 37458) compared with the chemical requirements of ASTM B409-06 (wt %)

Alloy 800H	Heat No. 37458	ASTM 409B-06
Ni	30.45	30.0–35.0
Cr	19.3	19.0–23.0
Fe	47.05	39.5 min.
Mn	1.31	1.5 max.
C	0.063	0.06–0.10
Cu	0.21	0.75 max.
Si	0.37	1.0 max.
S	0.001	0.015 max.
Al	0.43	0.15–0.6
Ti	0.45	0.15–0.6
Mo	0.21	—
Co	0.11	—

The specimen geometry used in this report for experimental strain rate jump tests, fatigue, and CF tests is shown in Figure 1. The specimen longitudinal direction is oriented along the rolling direction of the material plate. All the specimens were tested in the as-received condition.

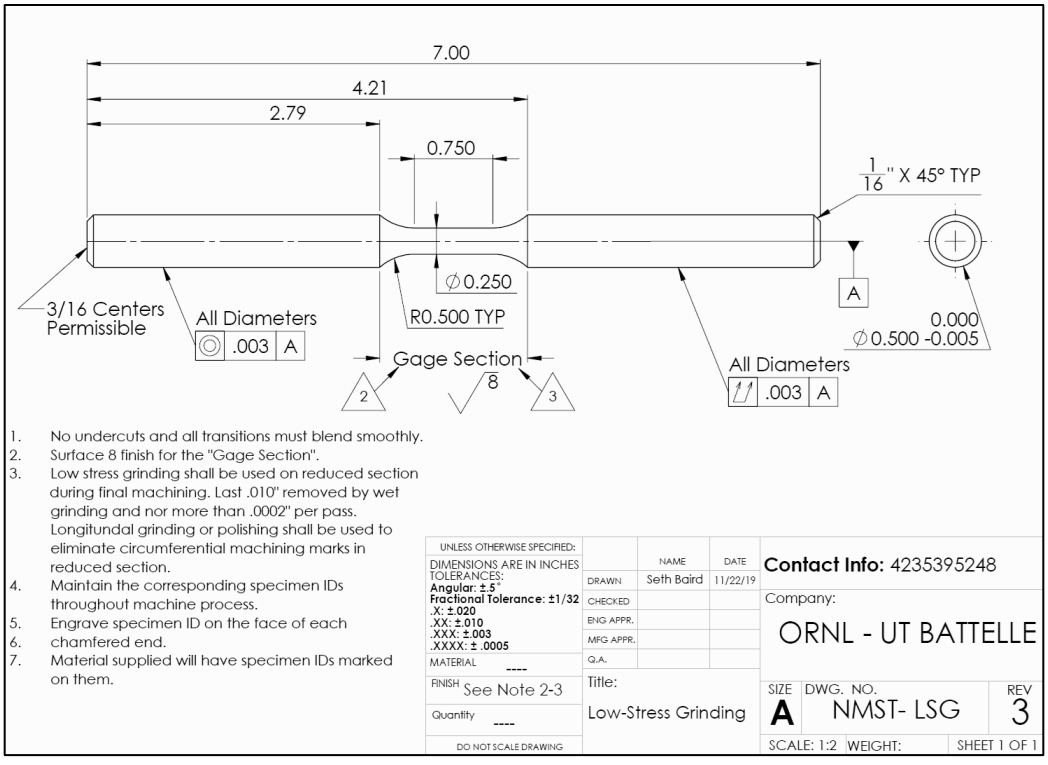

Figure 1. Standard fatigue and CF specimen geometry at Oak Ridge National Laboratory (ORNL). Dimensions are in inches.

3. EXPERIMENTS AND RESULTS

3.1 STRAIN RATE SENSITIVITY

The flow stress and strain rate at a constant temperature are related and typically given by the following empirical equation:

$$\sigma = C\dot{\varepsilon}^m, \tag{1}$$

where C is a material parameter, σ is the flow stress, $\dot{\varepsilon}$ is the strain rate, and m is the strain rate sensitivity exponent.

Instead of the displacement-controlled mode (Wright, et al. 2013), the tests performed in this study were under strain-controlled mode. The instantaneous change in flow stress corresponds to an instantaneous change in strain rate, and m is given as

$$m = \frac{log_{10}\left(\frac{\sigma_2}{\sigma_1}\right)}{log_{10}\left(\frac{\varepsilon_2}{\varepsilon_1}\right)}, \tag{2}$$

where the subscripts 1 and 2 indicate values of stress or strain immediately before and after the strain rate jump. Note that the true stress and true strain are used in Eq. (2). In this strain rate jump testing method, a finite amount of strain is required to produce a stable flow stress, and a consistent method for determining the strain rate sensitivity exponent, m, is necessary. Consistent with the method used in Wright et al. (2013), the stress σ_1, immediately before the strain rate jump, is directly obtained from experimental data, and the stress σ_2 is calculated based on an extrapolation line fitting the flow curve after an amount of plastic strain.

For this report, the strain rate sensitivity was experimentally determined by testing a single specimen on a servo hydraulic machine under strain-control mode at temperatures of 600°C, 700°C, and 800°C. The specimen was tensile loaded at a given strain rate until a steady-state flow stress was obtained, and then the strain rate was rapidly increased to obtain the flow stress at the next incremental strain rate. A schematic of applied strain rates in strain rate jump tests is presented in Figure 2. The changes in the slope of the strain vs. time plot correspond to when the strain rate instantaneously jumped to a higher rate. A total of five strain rates (i.e., 7.0×10^{-7}/s [R1], 7.0×10^{-6}/s [R2], 7.0×10^{-5}/s [R3], 7.0×10^{-4}/s [R4], and 7.0×10^{-2}/s [R5]) were performed in the strain ranges of 0%–0.5%, 0.5%–1.0%, 1.0%–1.5%, 1.5%–2.5%, and 2.5%–10%, respectively. Note that the segment R5 at 600°C has a lower target strain rate of 7.0×10^{-3}/s. The control extensometer has a nominal gage length of 12.7 mm.

Strain rate jump test results for Alloy 800H at temperatures of 600°C, 700°C, and 800°C are shown in Figure 3(a–c). These plots present true stress vs. true strain. The specimens were not tested to failure: testing was interrupted at about 10% total tensile strain. At 600°C and 700°C (in Figure 3a and b), an insignificant influence of strain rate in the flow stress can be found, suggesting a null strain rate sensitivity exponent (i.e., $m = 0$). Dynamic strain aging (DSA) behavior, evidently shown as the serrated flow in the stress–strain curves, was observed for the entire loading history at these two temperatures. The strain rate sensitivity exponents of Alloy 800H at 800°C were calculated using the method shown in Eq. (2). Strain rate sensitivity was observed at this test temperature, and higher strain rate introduced higher flow stress, as shown in Figure 3c. Furthermore, the results indicate that the DSA behavior depends on the applied strain rates and on the total deformation and that larger deformations suppress the DSA when

the strain rate is maintained. Systematic evaluation of the DSA behavior on Alloy 800H is beyond the scope of this report.

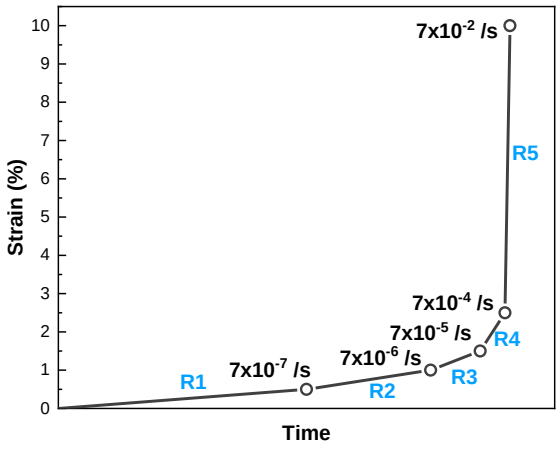

Figure 2. Schematic of the target strain rate in strain rate jump test.

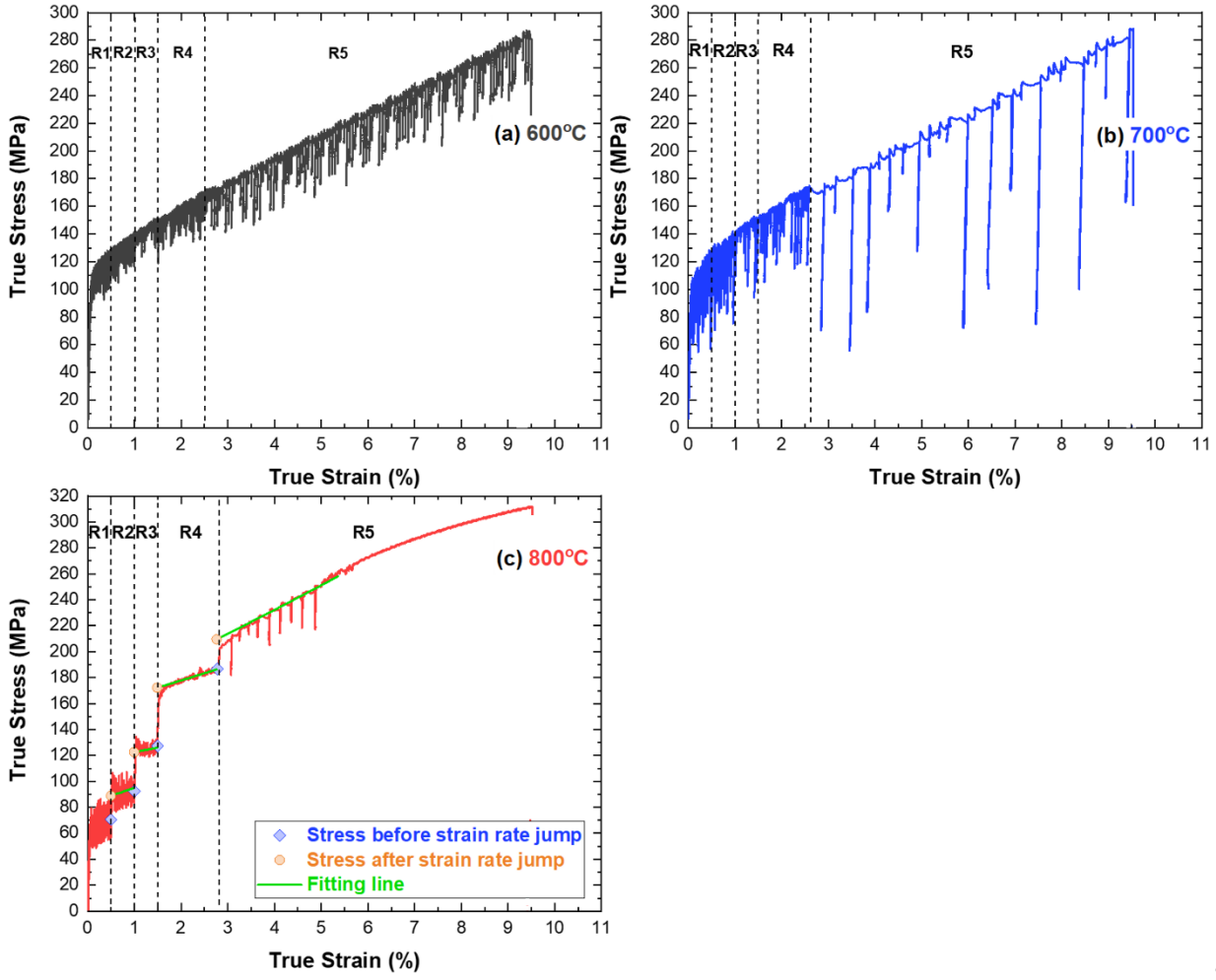

Figure 3. True stress–strain curves measured from strain rate jump testing at temperatures of (a) 600°C, (b) 700°C, and (c) 800°C.

The results of the strain rate sensitivity evaluation for Alloy 800H are summarized in Table 2 for all three tested temperatures.

Table 2. Calculated values of the strain rate sensitivity exponent as a function of strain rate for Alloy 800H at temperatures of 600°C, 700°C, and 800°C

Nominal strain rate (/s)	Temperature (°C)		
	600*	700	800
7×10^{-7} to 7×10^{-6}	0	0	0.101
7×10^{-6} to 7×10^{-5}	0	0	0.122
7×10^{-5} to 7×10^{-4}	0	0	0.131
7×10^{-4} to 7×10^{-2}	0	0	0.025

*Note: the actual strain rate for R5 at this temperature was performed at 7×10^{-3}/s.

3.2 FATIGUE TESTING AT STRAIN RANGE OF 0.8%

Strain-controlled pure fatigue tests to failure for Alloy 800H were conducted at various temperatures and followed the ASTM E606-12 standard. The strain rate was 1×10^{-3}/s. A triangular loading waveform with a fully reversed profile (i.e., loading ratio $R = -1$) was applied. The schematic of the loading profile for one cycle is presented in Figure 4. The control extensometer has a nominal gage length of 12.7 mm.

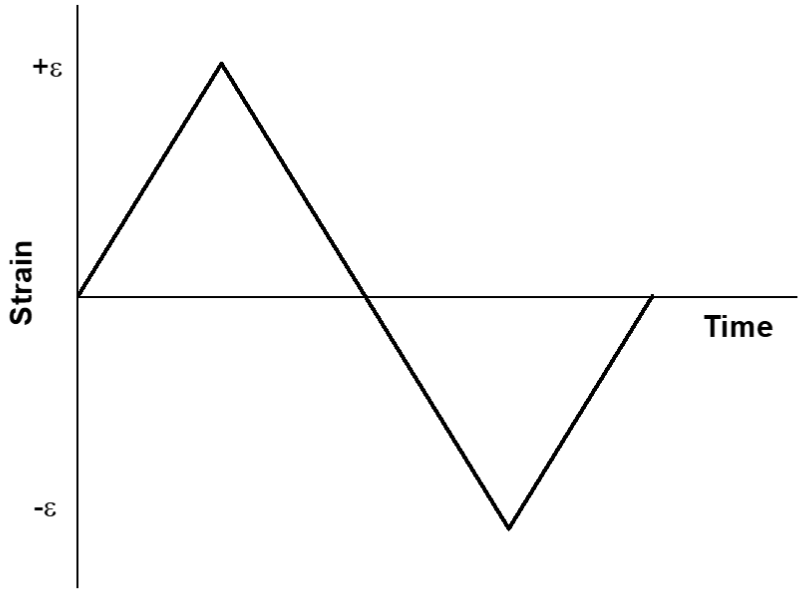

Figure 4. Strain-controlled fatigue loading profile for one cycle.

Six fatigue tests were performed at RT and at temperatures of 200°C, 400°C, 600°C, 700°C, and 800°C. All fatigue tests were performed at a nominal strain range of 0.8%. The fatigue testing parameter conditions, average strain range, inelastic strain at mid-life cycle, and cycles to failure are summarized in Table 3. The inelastic strains of these tests were evaluated, and the definition of the inelastic strain in a hysteresis loop is schematically illustrated in Figure 5. The failure criteria based on the 20% drop of the ratio between maximum and minimum stresses were used to determine the cycles to failure.

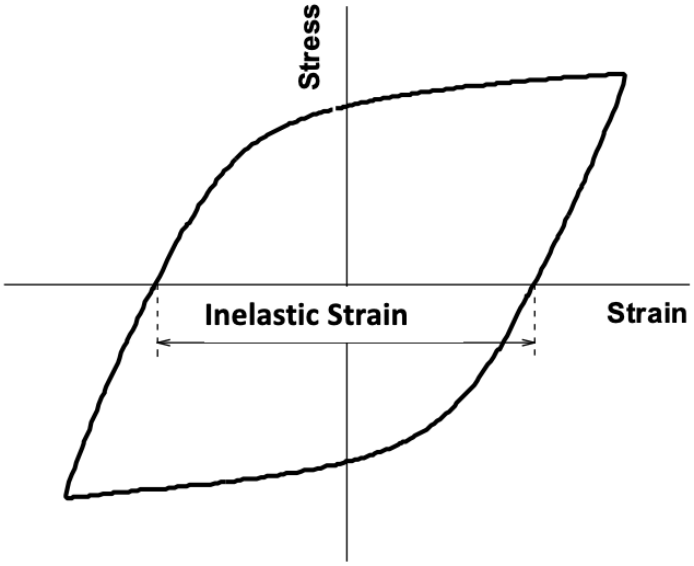

Figure 5. Schematic of the stress-strain hysteresis loop with the definition of inelastic strain.

Table 3. Fatigue test results for Alloy 800H at a nominal strain range of 0.8% at various temperatures

Specimen ID	Temperature (°C)	Average strain range (%)	Inelastic strain at mid-life (%)	Cycles to failure*
A800F14-01	23	0.734	0.427	14,436
A800F13-02	200	0.767	0.486	25,707
A800F16-03	400	0.747	0.387	11,466
A800F15-04	600	0.749	0.327	3,845
A800F17-05	700	0.741	0.346	1,631
A800F18-06	800	0.794	0.522	958

* Note: Failure criteria is defined as 20% drop in the ratio of maximum to minimum stress.

The maximum and minimum stresses as a function of the applied cycles of all the fatigue tests completed on Alloy 800H are plotted in Figure 6. Cyclic hardening behavior for the initial cycles was observed at all testing temperatures. The peak stresses decreased as the test temperature increased at the initial cycles. The characteristics of the material response to applied cyclic fatigue loading cycles were found to be very different at temperatures lower than 400°C compared with those at temperatures in the creep region (i.e., at temperatures of 600°C and above). The mechanism responsible for these different responses at different temperatures is beyond the scope of this study.

The hysteresis loops of all fatigue tests for cycle 10 and the midlife cycle are compared in Figure 7a and b, respectively. DSA behavior, shown as serrated flow upon yielding, was observed at 400°C and 600°C for all fatigue cycles. This behavior was observed for the initial cycles at higher temperatures (700°C and 800°C) but completely disappeared when more loading cycles were applied.

The width of the hysteresis loop indicates an effect of the test temperature on the development of the inelastic strains. Figure 8 presents the inelastic strains as a function of the applied cycles at different temperatures. At temperatures of 700°C and lower, the inelastic strain decreased sharply with additional applied cycles at approximately cycle 100, and then it gradually saturated until failure initiation. The inelastic strain at 800°C exhibited faster saturation at about 20 applied cycles.

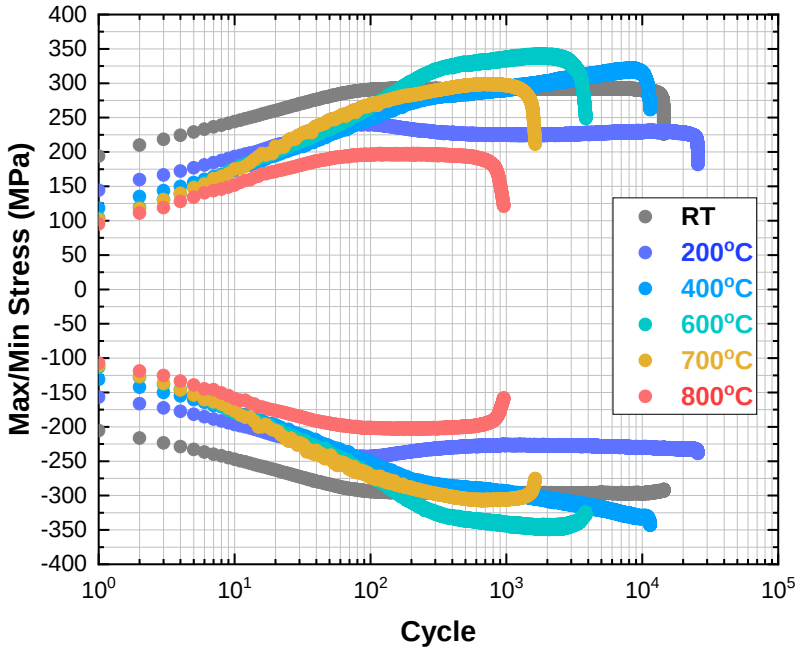

Figure 6. Maximum and minimum stresses as a function applied cycle for fatigue tests on Alloy 800H at nominal strain range of 0.8% at RT, 200°C, 400°C, 600°C, 700°C, and 800°C.

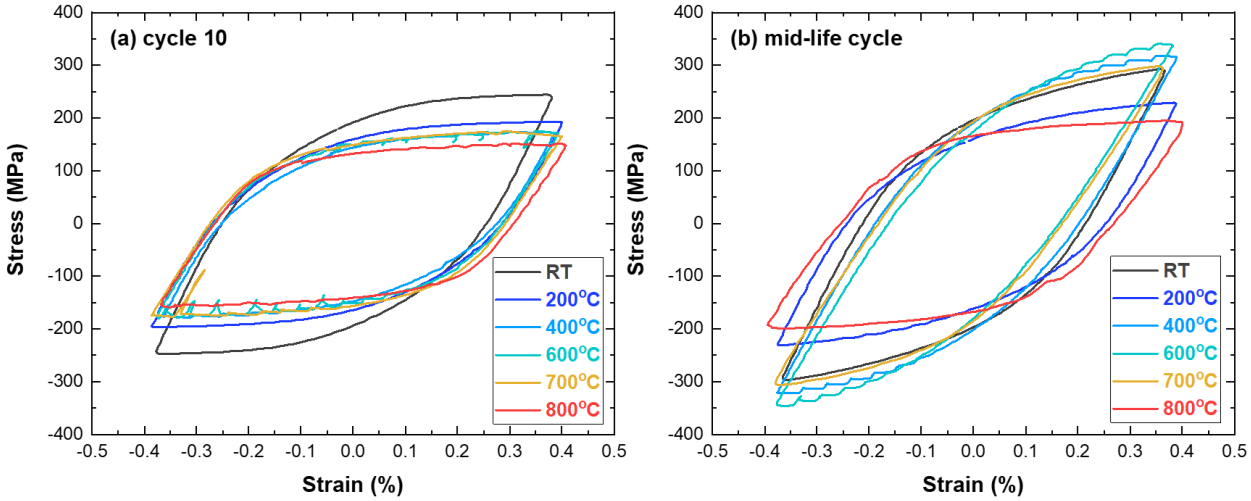

Figure 7. The hysteresis loops of midlife cycle of fatigue tests on Alloy 800H at strain range of 0.8% at RT, 200°C, 400°C, 600°C, 700°C, and 800°C.

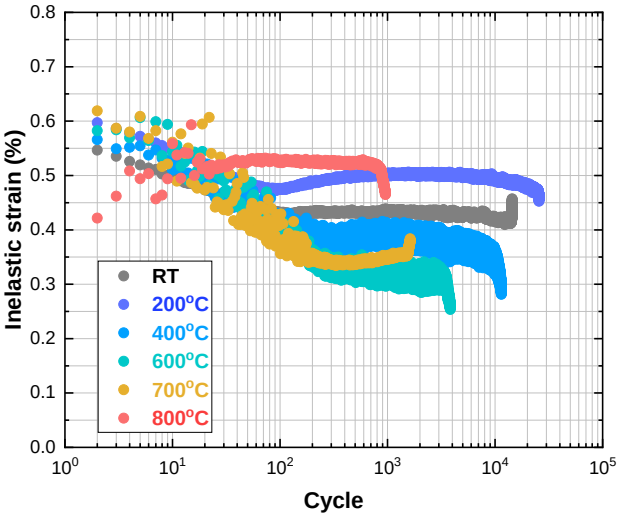

Figure 8. The inelastic strain as a function of applied cycle for fatigue tests on Alloy 800H at strain range of 0.8% at RT, 200°C, 400°C, 600°C, 700°C, and 800°C.

3.3 CYCLIC STRESS–STRAIN RESPONSE UNDER PURE FATIGUE LOADING

To probe the material's mechanical response to cyclic loading at different strain ranges and temperatures while supporting the material parameters for the development of the viscoplastic constitutive model, fatigue loading experiments were designed to collect key experimental information by applying a series of selected strain ranges (i.e., 0.2%, 0.3%, 0.6%, 0.8%, and 1.0% applied sequentially) on a single specimen with a finite number of cycles. The strain ranges were applied in an increasing loading sequence. The test temperatures were 650°C and 750°C. Note that the effect of loading history on the mechanical response of Alloy 800H under cyclic loading is neglected in this study.

Several cycles were applied to allow the peak stresses to reach a steady state. The straining profile for the strain-controlled fatigue testing segments is the same as that shown in Figure 4. The straining profile is a fully reversed profile (i.e., with a nominal straining ratio of $R = -1$). The nominal strain rate is 1×10^{-3}/s. The fatigue loading conditions are listed in Table 4.

Table 4. Specifically designed fatigue testing for Alloy 800H at 650°C and 750°C

Temperature (°C)	Nominal strain range* (%)	Tested cycles
650	0.2	400
650	0.3	400
650	0.6	400
650	0.8	400
650	1.0	400
750	0.2	400
750	0.3	400
750	0.6	400
750	0.8	400
750	1.0	250

*Note: this table has listed the applied strain ranges with a sequential order for each test temperature.

Figure 9 presents the maximum and minimum stresses as a function of the applied cycles for all fatigue loading strain ranges at 650°C. Results of all testing conditions indicated cyclic hardening behavior at the beginning of cycles, followed by the saturated maximum and minimum stresses. The magnitude of the peak stresses increased with increasing applied strain ranges. The hysteresis loops for cycle 10 and the last applied test cycle at different strain ranges are plotted in Figure 10a and b, respectively. The DSA occurred at higher strain ranges (i.e., 0.3%, 0.6%, 0.8%, and 1.0%). The DSA response persisted for all applied loading cycles at this temperature.

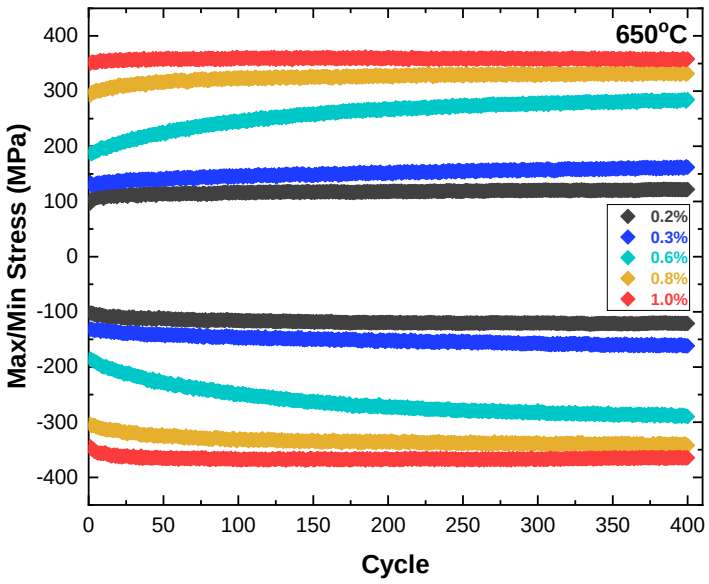

Figure 9. Maximum and minimum stresses as a function of applied cycle for the fatigue loading tests on Alloy 800H at 650°C.

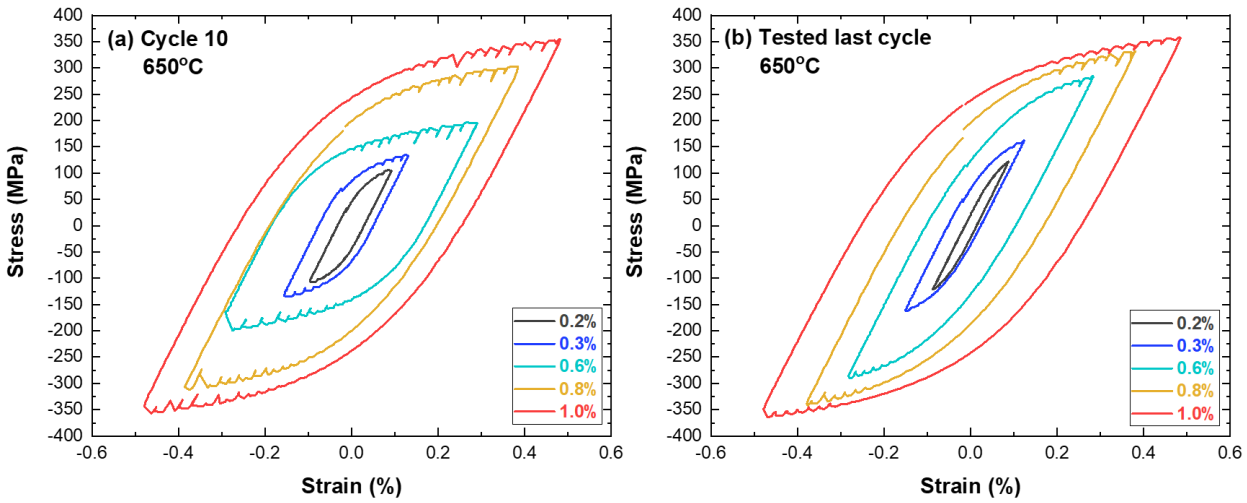

Figure 10. Hysteresis loops for (a) cycle 10 and (b) the last tested cycle of the fatigue loading tests on Alloy 800H at 650°C.

The maximum and minimum stresses as a function of the applied cycles at 750°C are shown in Figure 11. Like the results at 650°C, the maximum and minimum stresses increased within about 20 applied cycles for all the tested strain ranges before the saturation state, indicating a cyclic hardening behavior. The peak stresses increased with increasing applied strain range. At the high strain range of 1.0%, a slight softening trend of the maximum and minimum stresses was observed after 100 cycles, possibly indicating fatigue failure initiation.

The hysteresis loops at 750°C for cycle 10 and the last tested cycles at different strain ranges are plotted in Figure 12a and b, respectively. DSA response occurred only at 0.3% and 0.6% strain ranges for the initial applied cycles. As illustrated in Figure 12b, the last applied test cycles exhibit little or no evidence of DSA (i.e., DSA behavior is completely suppressed at this test temperature when additional loading cycles are applied).

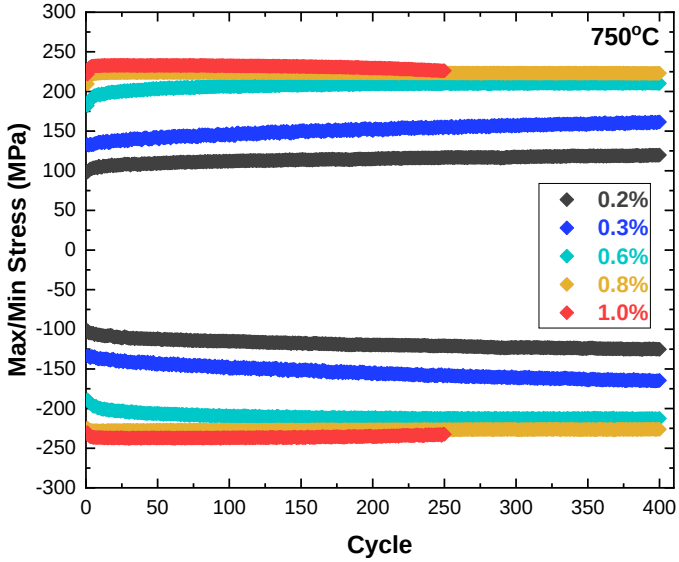

Figure 11. Maximum and minimum stresses as a function of applied cycle for the fatigue loading tests on Alloy 800H at 750°C.

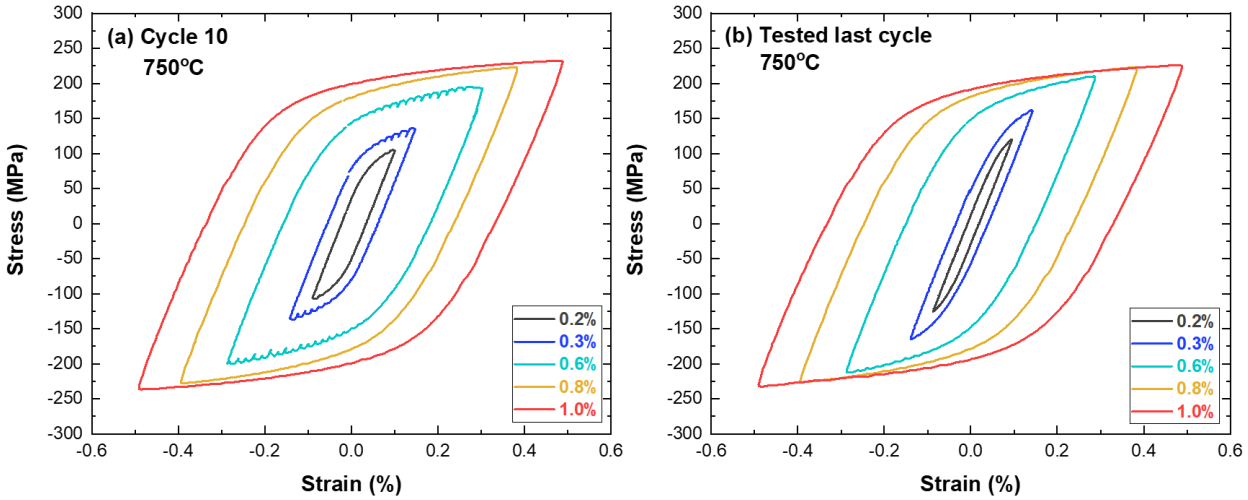

Figure 12. Hysteresis loops for (a) cycle 10 and (b) the last tested cycle of fatigue loading on Alloy 800H at 750°C.

3.4 CYCLIC RESPONSE UNDER CREEP-FATIGUE LOADING

Like the fatigue segment testing concept, CF experiments were designed to collect key experimental information by applying a series of selected strain ranges (i.e., 0.2%, 0.3%, 0.6%, 0.8%, and 1.0%) on a single specimen with tensile hold time of 600 s and a finite number of cycles. The test temperatures were also at 650°C and 750°C. The sequence of applied strain ranges at 650°C was 0.2%, 0.3%, 0.8%, 0.6%, and 1.0%, noting that the 0.6% strain range loading was unintentionally applied out of sequence after the 0.8% strain range loading. At 750°C, the applied strain ranges of 0.2%, 0.3%, 0.6%, 0.8%, and 1.0% were sequentially applied in increasing order. The effect of loading history on the mechanical response of Alloy 800H under CF loading was neglected in this study.

CF loading cycles were applied until steady state was achieved, evidenced by stabilized peak stresses as a function of the applied cycles. The strain profile for standard strain-controlled CF is shown schematically in Figure 13. The hold-time segment is applied to the maximum tensile strain amplitude. The strain profile is a fully reversed profile (i.e., with a nominal straining ratio of $R = -1$). The nominal strain rate is 1×10^{-3}/s. The control extensometer has a nominal gage length of 12.7 mm. The CF testing followed ASTM E2714-13 standard (ASTM 2013). The CF testing conditions are listed in Table 5.

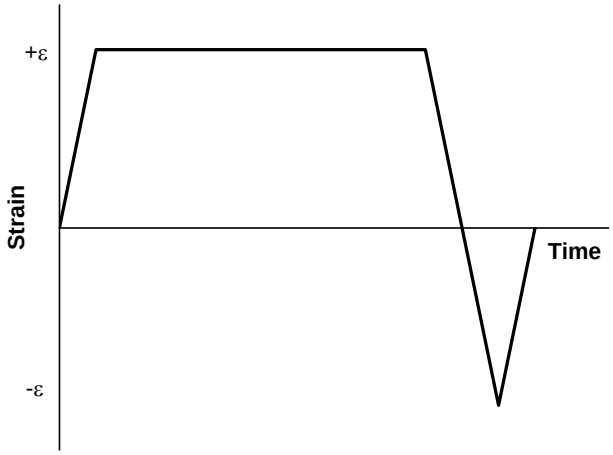

Figure 13. Strain-controlled creep-fatigue (CF) loading profile for one cycle.

Table 5. Specifically designed creep-fatigue testing for Alloy 800H at 650°C and 750°C..

Temperature (°C)	Nominal strain range* (%)	Tensile hold time (s)	Tested cycles
650	0.2	600	30
650	0.3	600	55
650	*0.8*	*600*	*80*
650	*0.6*	*600*	*100*
650	1.0	600	28
750	0.2	600	30
750	0.3	600	21
750	0.6	600	40
750	0.8	600	24
750	1.0	600	50

*Note: the 0.8% strain range CF at 650°C was performed before the 0.6% segment.

The maximum and minimum stresses of the CF loading cycles with different strain ranges at 650°C are compared in Figure 14. The unintentionally out-of-sequence loading segment at 0.6% strain range and the segment at 1% are plotted in Figure 14b. The maximum and minimum stresses measured under 0.6% strain range exhibit higher magnitude at initial cycles because preceding CF loading segment was at a higher strain range of 0.8%, evidently showing the loading sequence effect for the initial cycles. The hysteresis loops at 650°C for cycle 10 at 0.2%, 0.3%, and 0.8% strain ranges and those for the last tested cycles for all the applied strain ranges are plotted in Figure 15a and b, respectively. DSA is not evident after 10 cycles.

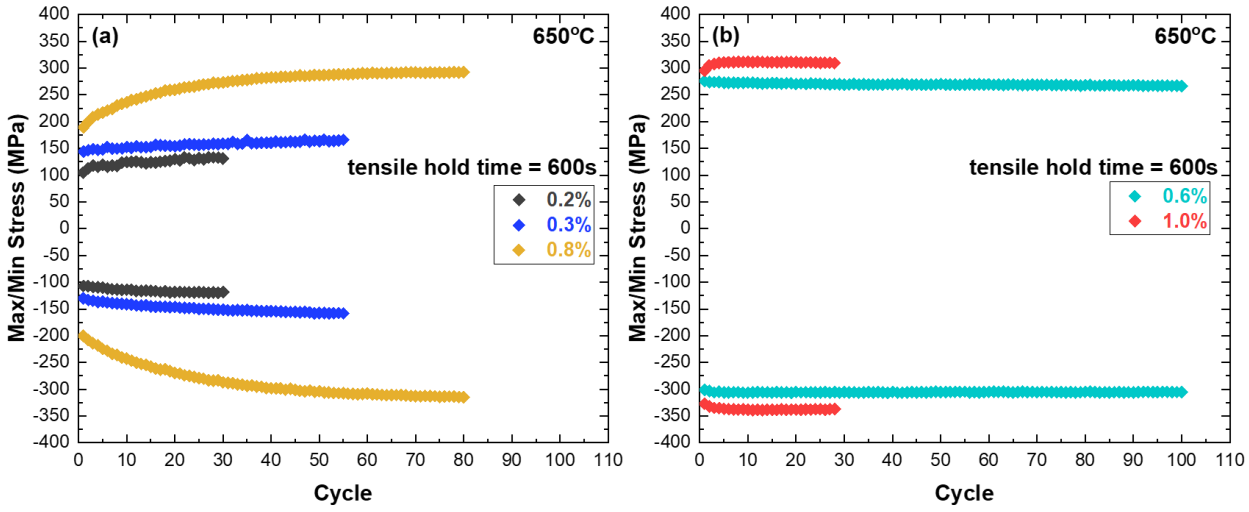

Figure 14. Maximum and minimum stresses as a function of applied cycle for the CF tests on Alloy 800H at 650°C at strain ranges of (a) 0.2%, 0.3%, and 0.8% and (b) 0.6% and 1.0%.

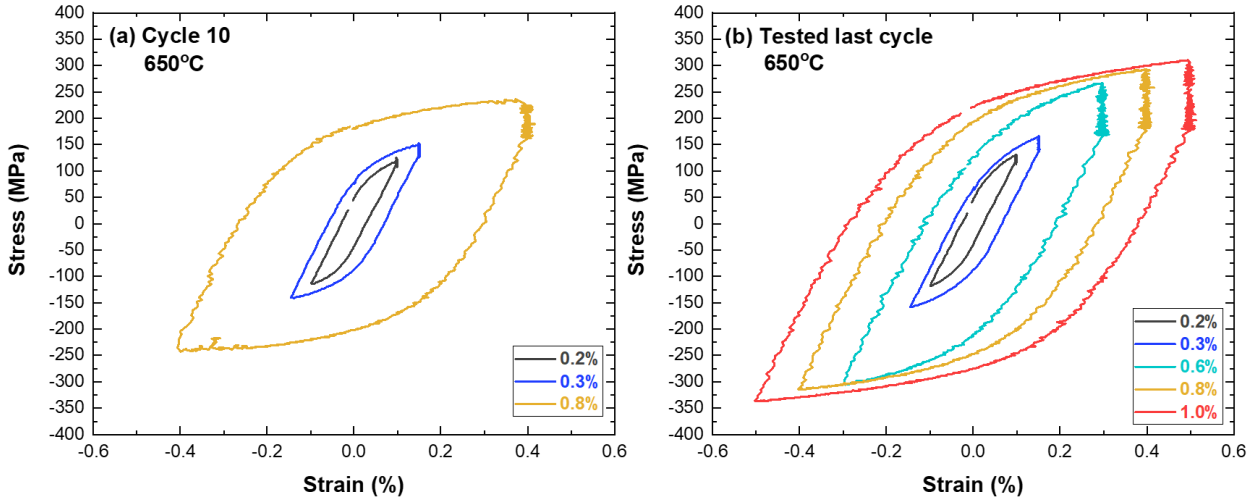

Figure 15. Hysteresis loops for (a) cycle 10 at strain ranges of 0.2%, 0.3%, and 0.8%, and (b) the last tested cycles for all the strain ranges of the CF tests on Alloy 800H at 650°C.

The evolutions of maximum stresses as a function of applied cycle at 650°C at the beginning of the hold time and of the relaxed stresses at the end of the hold time are presented in Figure 16. Figure 17 presents the stress relaxation curves of cycle 10 and of the last applied test cycles as a function of the hold time. The stress relaxation curves are also normalized by the stresses at the beginning of the tensile hold and are compared in this figure. The amount of stress relaxation is small at relatively low strain ranges of 0.2% and 0.3%, and only relaxed approximately 10% at the end of the hold time. At strain ranges of 0.6% and above, the stresses relaxed much faster during the tensile hold: stress dropped by approximately 35% after the 600 s tensile hold during the last applied test cycles.

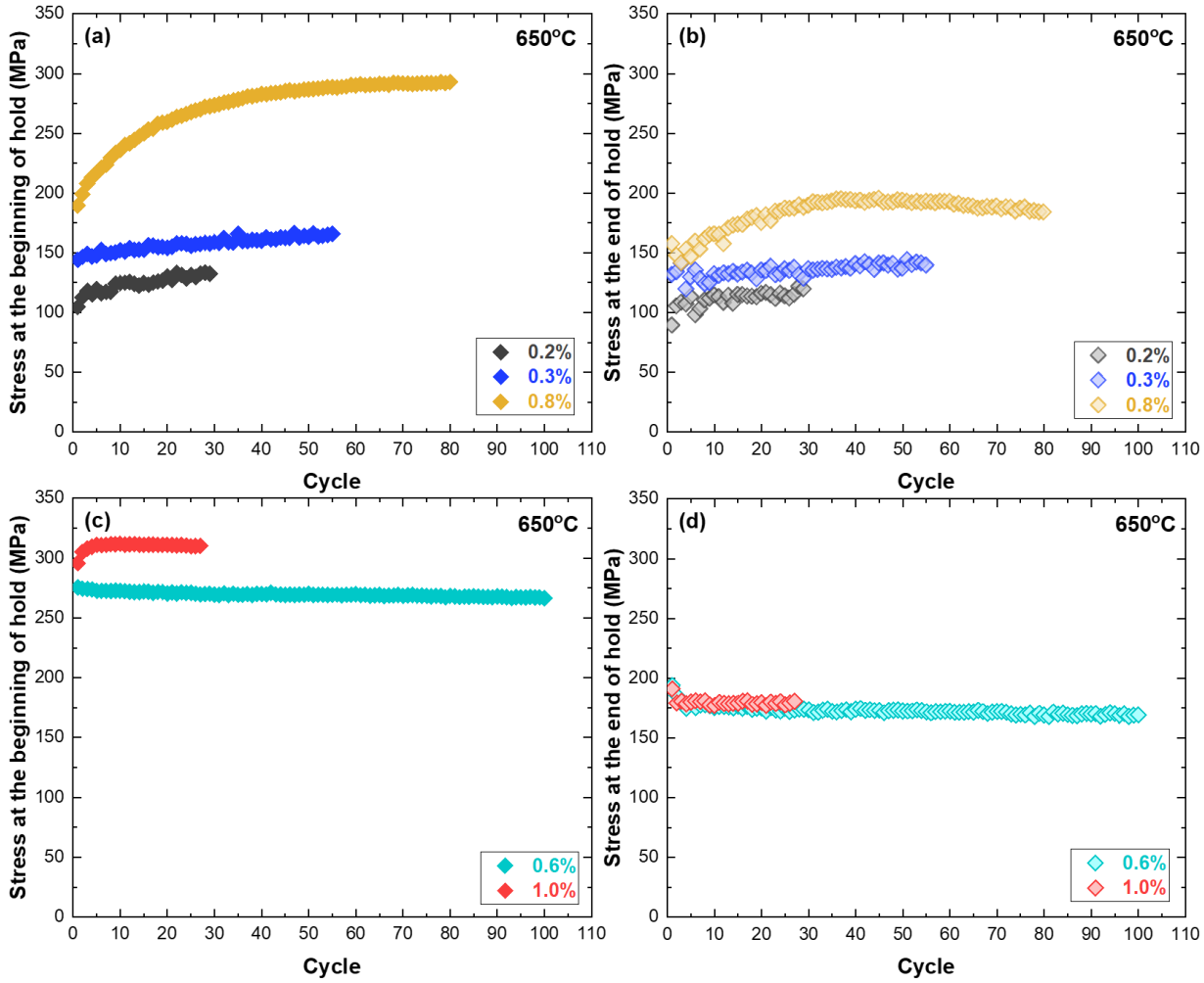

Figure 16. Evolution of the stresses at the beginning and the end of the hold time during the CF tests on Alloy 800H at 650°C for strain ranges of (a, b) 0.2%, 0.3%, and 0.8% and (c, d) 0.6% and 1.0%.

For the CF loading cycles at 750°C, Figure 18 shows the maximum and minimum stresses of all sequential CF loading segments. All testing segments achieved steady state and saturated peak stresses. The hysteresis loops at 750°C for cycle 10 and the last applied test cycles at different strain ranges are plotted in Figure 19a and b, respectively. Little or no DSA is evident in flow stresses after 10 cycles.

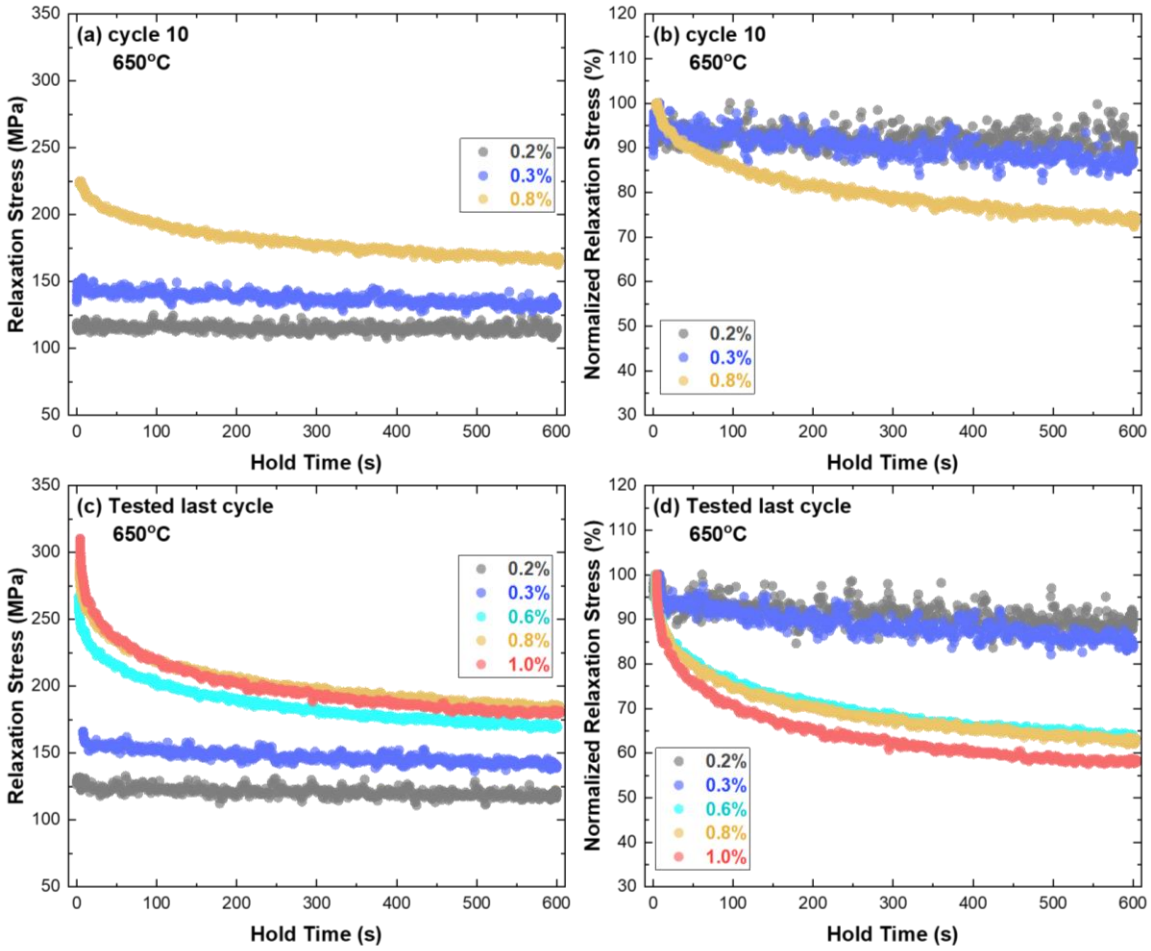

Figure 17. Stress relaxation curves and the normalized stress relaxation curves of cycle 10 at strain ranges of (a, b) 0.2%, 0.3%, and 0.8% and (c, d) those of the last tested cycles for all strain ranges of the CF tests on Alloy 800H at 650°C.

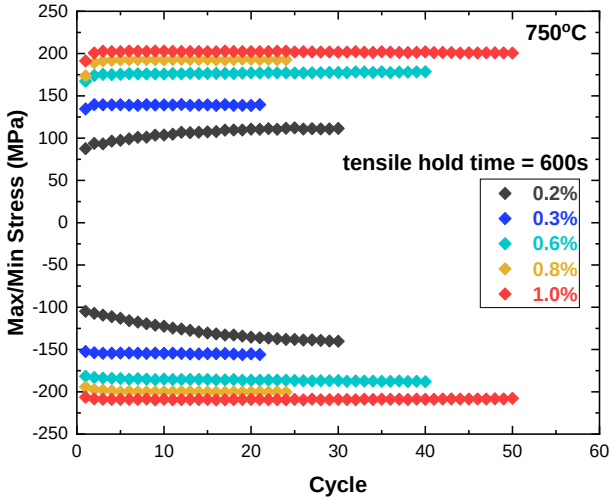

Figure 18. The maximum and minimum stresses as a function of applied cycle for the specifically designed CF test on Alloy 800H at 750°C.

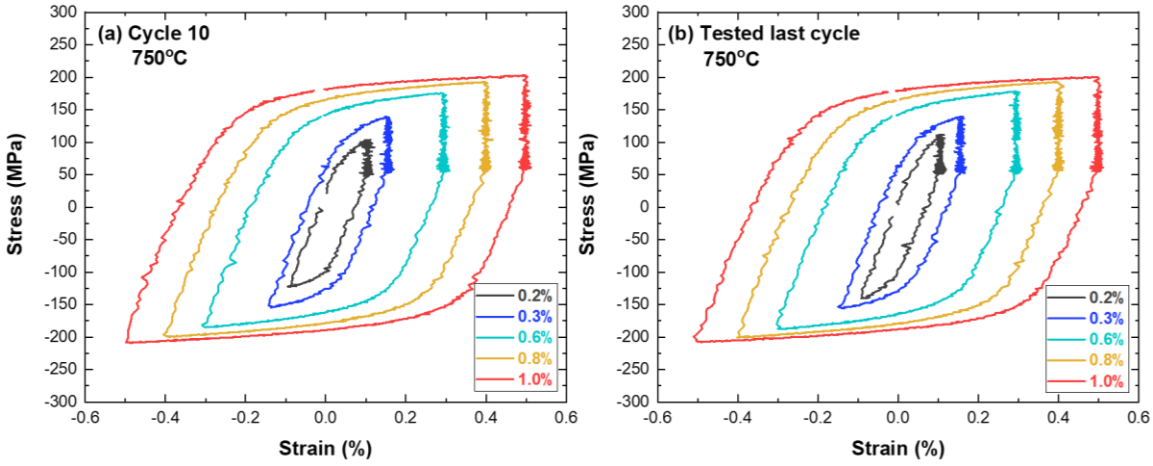

Figure 19. The hysteresis loops for (a) cycle 10 and (b) the last tested cycle of the specifically designed CF test on Alloy 800H at 750°C.

The evolutions of maximum stresses as a function of applied cycle for all CF testing results at 750°C at the beginning of the tensile hold and of the relaxation stresses at the end of the hold are presented in Figure 20. Despite significant differences in the maximum stress at the beginning of the hold, as shown in Figure 20a, the relaxation stresses at the end of the hold are comparable to each other. As the strain range increases from 0.2% to 0.6%, more significant stress relaxation occurs, but saturation is evident when the strain range is beyond 0.6%. At strain ranges of 0.6% and above, the stress relaxes by about 70% at the end of the tensile hold after about 10 cycles. The stress relaxation curves and the normalized stress relaxation curves of cycle 10 and the last applied test cycles are presented in Figure 21. The stress relaxation behavior at strain ranges of 0.6%, 0.8%, and 1.0% is nearly identical: an approximately 60% stress drop occurs after a 60 s tensile hold at this test temperature.

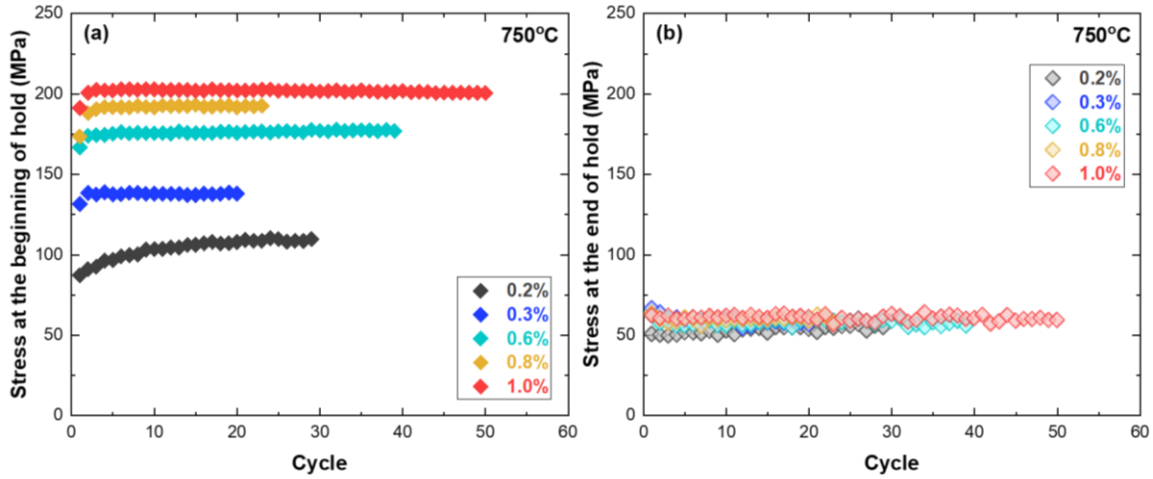

Figure 20. The evolutions of maximum stresses and relaxation stress as a function of applied cycle (a) at the beginning and end of the hold, respectively, and (b) the normalized relaxation stress of the specifically designed CF test on Alloy 800H at 750°C as a function of applied cycle.

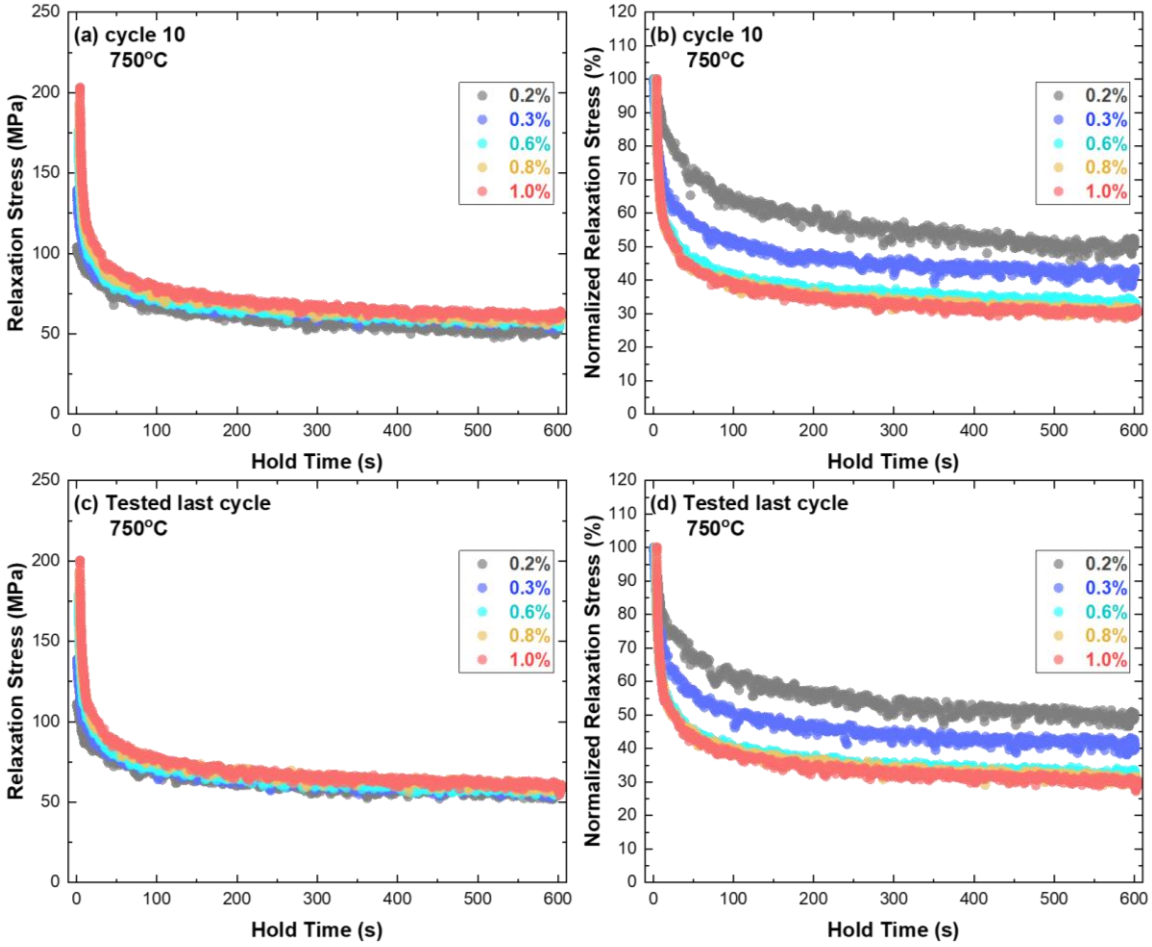

Figure 21. The stress relaxation curves of (a) cycle 10 and (c) the last tested cycle, respectively. The normalized stress relaxation curves of (b) cycle 10 and (d) the last tested cycle of the specifically designed CF test on Alloy 800H at 750°C.

4. SUMMARY

In support of the development of the viscoplastic constitutive model for use of inelastic analysis methods in Section III, Division 5 of the ASME Boiler and Pressure Vessel Code, specific experiments were designed to evaluate the mechanical responses of Alloy 800H. Strain rate jump tests, fatigue failure tests, and cyclic responses under fatigue and CF loading were performed at various temperatures at ORNL. The results are summarized as follows.

- The influence of strain rate on the flow stress is insignificant at temperatures of 600°C and 700°C for Alloy 800H, whereas it exhibits significant strain rate sensitivity at 800°C.

- The fatigue responses at the nominal strain range of 0.8% exhibited different deformation mechanisms at temperatures lower than 600°C compared with test temperatures in the creep region.

- Alloy 800H exhibited cyclic hardening behavior at all tested temperatures. The DSA behavior was observed in all the test cycles in pure fatigue tests at temperatures of 400°C and 600°C and in specifically designed segment fatigue loading at temperatures of 650°C. This DSA behavior depends on the test temperature, the cyclic loading strain range, the number of the applied cycles, and the total deformation.

- The results from the sequential CF loading at the higher test temperature of 750°C indicate that the stress relaxation behavior was nearly identical at large strain ranges (i.e., 0.6% and above) despite the differences in the maximum stresses at the beginning of the tensile hold.

REFERENCES

ASME. 2019a. *Boiler and Pressure Vessel Code, Section III Division 5, Rules for Construction of Nuclear Facility Components, Subsection HB Subpart B,* American Society of Mechanical Engineers, New York (2021 Edition).

ASTM B409-06. 2016. *Standard Specification for Nickel-Iron-Chromium Alloy Plate, Sheet, and Strip,* ASTM International, West Conshohocken, Pennsylvania, www.astm.org.

ASTM E606/E606M-21. 2021. *Standard Test Method for Strain-Controlled Fatigue Testing,* ASTM International, West Conshohocken, Pennsylvania, www.astm.org.

ASTM E2714-13. 2020. *Standard Test Method For Creep-Fatigue Testing,* ASTM International, West Conshohocken, Pennsylvania, www.astm.org.

Wright, J. K., Wright, R. N., and Sham T.-L., 2010, *Next Generation Nuclear Plant Steam Generator and Intermediate Heat Exchanger Materials Research and Development Plan*, INL/EXT-08-14107 Rev. 1, Idaho National Laboratory, Idaho Falls, Idaho.

Wright, J. K., Simpson, J. A., Wright, R. N., Carroll, L. J., and Sham, T. -L., 2013, "Strain rate sensitivity of alloys 800h and 617," in *Pressure Vessels and Piping Conference* 55638, V01AT01A053. American Society of Mechanical Engineers.